UdeM-LPN-TH-115-92

Fermilab Library
0 1160 0019247 0

deM-LPN-TH-115-92

32

PHYSICS BEYOND THE STANDARD MODEL AT e^+e^- LINEAR COLLIDERS

A. DJOUADI

Deutsches Elektronen–Synchrotron DESY, D–2000 Hamburg 52, Germany
and
Laboratoire de Physique Nucléaire, Université de Montréal, H3C 3J7 Canada

and

P. M. ZERWAS

Deutsches Elektronen–Synchrotron DESY, D–2000 Hamburg 52, Germany.

ABSTRACT

The physics potential of e^+e^- linear colliders which in a first phase will operate in the energy range between 300 and 500 GeV, is described in this report. Two aspects are emphasized: (i) Precision measurements in the heavy particle sector of the Standard Model can hold clues to the physics beyond the Standard Model, in particular the electroweak properties and rare decay modes of the top quark, and the triple and quartic self–couplings of the electroweak bosons. (ii) New vector bosons and novel matter particles which are predicted by extended gauge theories, can be searched for and studied in detail. The machines are ideal for exploring supersymmetric extensions of the Standard Model, the $\mathcal{SUSY}$ Higgs spectrum and the supersymmetric partners of [non–colored] gauge/Higgs bosons and leptonic matter particles.

1 Introduction

1.1 The Physical Basis

The e^+e^- colliders which have operated over the past two decades have been outstandingly successful in searching for the fundamental constituents of matter, and in exploring their interactions. The charm quark and the τ lepton were established at SPEAR, completing the second family and opening up the third. The gluons were identified as the force quanta of the strong interactions at PETRA. Besides the discovery of these new particles, the copious production of quarks and leptons in a clean experimental environment has allowed precise studies of their electroweak properties. Crowning an exciting experimental evolution over many years, the present high-precision analysis of the Z boson and its decay modes at LEP has laid a solid base for both the electroweak as well as the strong sector of the Standard Model.

The next generation e^+e^- colliders [1] will be important instruments for the search of new particles which are predicted by all theoretical approaches to the physics beyond the Standard Model ($\mathcal{SM}$) [2, 3]. Even the particles in the $\mathcal{SM}$ may hold important clues to this new physics domain. In particular the interactions of the heavy particles, the top quark and the electroweak vector bosons, could be sensitive to non-$\mathcal{SM}$ effects [2, 3].

Top quark. The mass of the top quark is apparently greater than that of the electroweak gauge bosons. Understanding the role of this particle in Nature is therefore an important goal for the future. A scan of the $t\bar{t}$ threshold region will allow the measurement of the top quark mass to better than 500 MeV. This is a particularly desirable goal since we expect future theories of flavor dynamics to predict relations among the fermion masses in which the heavy top quark plays a key role. Helicity analyses of the $t\bar{t}$ production vertex and of the t decay vertex will lead to constraints of a few percent on the magnetic dipole moments of the top quark and the chirality of the charged (tb) decay current. The $\mathcal{CP}$ violating electric dipole moments can be probed to less than 3×10^{-18} ecm. Last but not least, the top quark may have unusual decay modes in extensions of the Standard Model, decays to charged Higgs bosons or top decays to stop. These decay modes are expected to be rare, yet frequent enough to be analyzed thoroughly in e^+e^- colliders.

W, Z Bosons. To study the dynamics of the electroweak gauge bosons is another important task of high energy e^+e^- colliders. The form and the strength of the triple and quartic couplings of these particles are uniquely prescribed by the gauge symmetries. The triple gauge boson couplings define the electroweak charges, the magnetic dipole moments and the electric quadrupole moments of the W bosons in the static limit. Anomalous couplings would appear, for example, in scenarios with non-pointlike and dynamically generated W and Z bosons. By destroying the unitarity cancellations which in the $\mathcal{SM}$ are associated with the longitudinal degrees of freedom of the gauge bosons, any small deviations from the $\mathcal{SM}$ values will be magnified with increasing energies and the bounds will tighten. If all parameters are allowed to vary freely, the anomalous magnetic dipole and electric quadrupole moments can be probed to less than about $\pm$ 0.02.

Even though present experimental data support the Standard Model to unprecedented levels of accuracy, extensions can nevertheless be anticipated theoretically. Two directions are particularly important.

Extended Gauge Models. It is physically plausible that the Standard Model, based on the gauge symmetry group $SU(3)_C \times SU(2)_L \times U(1)_Y$, will be embedded into a grand unified theory at very high energies $\sim 10^{16}$ GeV. The symmetry groups of these theories may be broken down to the $\mathcal{SM}$ group in several steps. In this case new gauge bosons are predicted with masses which eventually may not be far away from the scale of electroweak symmetry breaking. If the e^+e^- energy can be raised high enough, the machine will operate as a Z' factory. If the masses are above the maximum energy, the exchange of virtual Z' particles affects the production cross sections and the forward-backward asymmetries. At $\sqrt{s} = 500$ GeV, these observables are sensitive to any Z' exchange up to masses of order 3 to 4 TeV. The various models can be discriminated and their parameters can be measured with sufficiently high accuracy for boson masses up to $\sim$ 2 TeV. In most of the unifying groups additional new fermions are predicted with masses which may not be much larger than the Fermi scale. Among these novel leptons and quarks with exotic $\mathcal{SM}$ quantum numbers, heavy neutrinos, possibly of Majorana type, are a prominent example. These particles can either be produced pairwise or, if the mixing is strong enough, in association with ordinary chiral $\mathcal{SM}$ particles. While masses up to the beam energy are accessible in pair production, the total energy can be fully exploited in associated production of heavy new fermions with light $\mathcal{SM}$ fermions. Many other novel particle species, if realized in Nature, can be investigated in e^+e^- colliders, leptoquarks, particles associated with non-conventional electroweak symmetry breaking, *etc.*

Supersymmetry. An attractive extension of the Standard Model is provided by supersymmetry ($\mathcal{SUSY}$), which stabilizes moderate masses of Higgs particles in the context of high energy scales demanded by grand unified theories. Supersymmetric theories predict a greatly extended Higgs sector, scalar partners of the $\mathcal{SM}$ fermions as well as spin 1/2 partners to the gauge bosons and Higgs particles. While the colored $\mathcal{SUSY}$ partners, squarks and gluinos, can be produced at high rates in hadron colliders, e^+e^- colliders are ideal machines to search for the Higgs particles, the sleptons and the non-colored gauginos and Higgsinos. If R parity is conserved – an assumption which may be relaxed – sleptons and gauginos/Higgsinos are produced pairwise in e^+e^- collisions so that mass spectra up to the beam energy can be covered. Besides the Higgs particles, gauginos and Higgsinos are expected to be the lightest among the $\mathcal{SUSY}$ particles, followed by the sleptons. The search for these $\mathcal{SUSY}$ states therefore provides one of the prime motivations for operating e^+e^- linear colliders.

While new high-mass vector bosons and particles carrying color quantum numbers can be searched for in hadron colliders, e^+e^- colliders are in many ways unique in their ability to detect and explore non-colored particles such as novel leptons and non-colored supersymmetric particles, sleptons and gauginos/Higgsinos. In addition, e^+e^- colliders are ideal machines for the search of Higgs particles in the intermediate mass range and the exploration of their properties. If new neutral gauge bosons were within the reach of the collider, the machine would naturally develop into a factory for these particles.

1.2 Characteristics of the Colliders

Since the synchrotron radiation in circular machines rises as the fourth power of the energy, e^+e^- colliders beyond LEP200 must be linear machines to avoid prohibitive energy losses. This type of accelerator that has been pioneered by the SLC. The machines will probably be realized in two phases. In the first phase the energy range above LEP200 up to ~ 500 GeV will be covered, in the second phase an energy of about 1 to 2 TeV will be reached. The physics potential of e^+e^- linear colliders in the first phase between 300 and 500 GeV is complementary to that of the high-energy proton colliders, covering areas in an ideal manner, which are very difficult to explore in hadron colliders. In the second phase the energy of the machines becomes effectively equivalent to the proton colliders. Various reference designs are being studied at DESY-Darmstadt, SLAC, KEK and Novosibirsk based on conventional acceleration techniques, while TESLA exploits superconducting technologies and CLIC is a novel two-beam linear accelerator [1].

The cross sections of most of the reactions which will be investigated at e^+e^- linear colliders, are of the order of the μ-pair cross section $e^+e^- \to \mu^+\mu^-$. Given a luminosity $\mathcal{L} = 10^{33}$ cm^{-2} sec^{-1} and an effective year of running time taken as 10^7 sec, the accumulated luminosity $\int \mathcal{L} = 10$ fb^{-1} leads to the production of about 5,000 μ pairs at a c.m. energy of 500 GeV. Such an integrated luminosity proves sufficient to allow for thorough data analyses, including cuts on the event samples and allowing for acceptance losses in the detectors. To generate the same number of events at higher e^+e^- energies, the luminosity must be scaled up as the square of the energy.

The required high luminosity will be achieved by squeezing the electrons and positrons into bunches of extremely small transverse dimensions. Due to the large electromagnetic fields at these small distances, the trajectories of the electrons traversing the positron bunch – and vice versa – are bent so that the particles emit synchrotron light during the bunch collisions (beamstrahlung). As a result, a fraction of the beam energy is lost and the initially sharp e^+e^- c.m. energy is smeared out. However, in narrow-band-beam designs, these effects can be reduced to the level of a percent and less [4]. The colliding beamstrahlung photons produce background e^+e^- pairs, concentrated to cones of half-aperture $\sim 10°$ about the beam pipe. The colliding photons will also produce hadrons, but at a level in narrow-band-beam designs that is of the same order as the rate induced by the ordinary γ bremsstrahlung. Only a very small fraction of e^+e^- annihilation events need eventually be discarded due to contamination by underlying $\gamma\gamma$ events.

By illuminating the incoming electron and positron bunches by laser light, hard Compton back-scattering of the laser photons off the electrons and positrons can be exploited to transform e^+e^- colliders into $e\gamma$ and $\gamma\gamma$ colliders [5]. With the overall luminosity in size comparable to the original e^+e^- luminosity, the $e\gamma$ spectrum is strongly peaked at about 90% of the total e^+e^- energy. The distribution of the $\gamma\gamma$ invariant energies is broader, yet by using polarized beams it can be strongly enhanced near the maximum of 80% of the total e^+e^- energy. There is a broad spectrum of physics problems which can be addressed in $e\gamma$ and $\gamma\gamma$ colliders. Prominent examples are the measurement of the Higgs coupling to two photons, precision studies of the electromagnetic couplings of the W bosons and the production of selectrons with masses beyond the $e^\pm$ beam energies.

2 Non-Standard Physics of Standard Particles

2.1 Top Quark

Top quarks are the heaviest matter particles in the 3-family Standard Model. The non-observation of top quarks at the Tevatron leads to a lower limit of 91 GeV for the t mass, while the evaluation of radiative corrections for the electroweak observables measured with high precision at LEP and elsewhere, suggests a top mass in the range $m_t = 140 \pm 30$ GeV.

Since the top quark is a particle of exceptionally large mass, many interesting channels could open for phenomena beyond the $\mathcal{SM}$ domain. Helicity and polarization analyses [6, 7, 8] can shed light on anomalous magnetic [and electric] dipole moments of the top quark, as well as on non-standard RH current admixtures to the decay amplitude. In the supersymmetric extension of the $\mathcal{SM}$, top decays to charged Higgs [9], $t \to b + H^+$, and top decays to stop plus the lightest neutralino [10], $t \to \tilde{t} + \tilde{\gamma}$, could be of interest. Additional non-standard heavy quark multiplets could lead to FCNC decays of top quarks [11], $t \to c + Z$ for instance, as the mixing between quarks increases with the mass, thus favoring the heavy (t, c) pair sector. Naturally, this listing cannot be complete and other exciting phenomena may emerge in the future.

The main production mechanism for top quarks in e^+e^- collisions [12] is the annihilation channel $e^+e^- \to Z, \gamma \to t\bar{t}$. For a top mass $m_t = 150$ GeV the maximum of the cross section is reached about 25 GeV above the threshold and a rate of $\sim 10,000$ top quark pairs is generated for an integrated luminosity $\int \mathcal{L} = 10$ fb^{-1}. This is just about the same number of top quarks that can be used for physics analyses in pp colliders like LHC [13] after filtering the top quarks out of the background. In the clean environment of e^+e^- colliders, the top quarks are easily isolated [8]. The sharp rise of the $t\bar{t}$ cross section at threshold, caused by the production of toponia and their remnants, will allow a high-precision measurement of the top mass to better than 500 MeV.

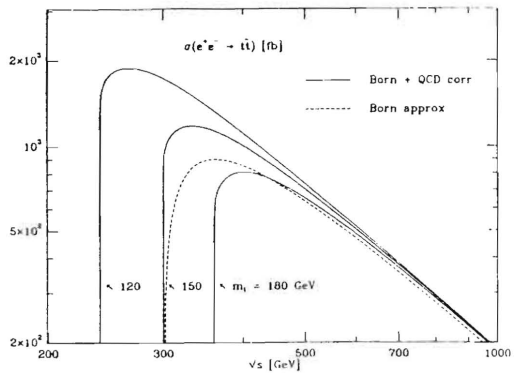

Fig. 1 The cross section $\sigma(e^+e^- \to t\bar{t})$ [including QCD corrections] for three values of the top mass [12].

2.1.1 Static t Parameters

Because of the large t mass, deviations from the $\mathcal{SM}$ may manifest themselves in the top quark sector first. Examples in which the large mass is crucial, are provided by multi-Higgs doublet models, models of dynamical symmetry breaking and compositeness. These effects can globally be described by form factors parametrizing the electroweak $t\bar{t}$ production current ($a = \gamma, Z$) and the weak (t, b) decay current ($a = -$) [7],

$$j^a_\mu = F^a_{1L}\gamma_\mu P_L + F^a_{1R}\gamma_\mu P_R + \frac{i\sigma_{\mu\nu}q_\nu}{2m_t}[F^a_{2L}P_L + F^a_{2R}P_R] \tag{1}$$

[$P_{L,R}$ project on the left and right chirality components of the wave functions.] In the $\mathcal{SM}$, $F^-_{1L} = 1$ while all other F^-_i vanish; $F^\gamma_{1L} = F^\gamma_{1R} = 1$ and $F^\gamma_{2L} = F^\gamma_{2R} = 0$, analogously for the Z current. $\mathcal{CP}$ invariance requires $F^{\gamma,Z}_{2L} = F^{\gamma,Z}_{2R}$ in the $t\bar{t}$ production current, and equal phases for F^-_{1L} and F^-_{2R} *etc.* in the decay current. The static values of the form factors $F^{\gamma,Z}_2$ are the anomalous magnetic and electric dipole moments of the top quark. The form factors are determined experimentally by measuring the angular distribution of the $t\bar{t}$ decay products, $e^+e^- \to t\bar{t}, t \to bW^+, W^+ \to f\bar{f}'$ *etc.* The corresponding helicity amplitudes have been given in [7] at the quark level. This requires that the top quark can be treated as a free particle, the polarization of which not being affected by non-perturbative hadronic binding effects. This assumption is justified by the short lifetime of the top quark. While the general helicity analysis can be found in the literature, we shall focus here on a few physically interesting specific examples.

(a) Anomalous magnetic dipole moments of the top quark

If the electrons in $e^+e^- \to t\bar{t}$ are left-handedly polarized, the top quarks are preferentially produced as left-handed particles in the forward direction and only a small fraction is produced as right-handed particles in the backward direction. As a consequence of this $\mathcal{SM}$ prediction, the backward direction is most sensitive to small anomalous magnetic moments of the top quarks. This is demonstrated quantitatively in Fig. 2 where the angular distribution of the top quarks is broken down to various helicity contributions. It is apparent that the anomalous magnetic moments can be probed to a few percent through the measurement of the angular dependence of the t quark cross section.

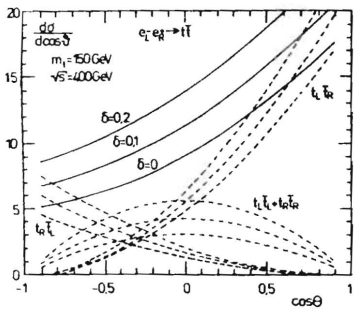

Fig. 2 Angular distributions of the t production cross section for fixed t and $\bar{t}$ helicities in polarized $e^-_L e^+_R$ annihilation. The parameter δ measures the anomalous magnetic (γ, Z) dipole moment of the top quark; from Ref. [14].

(b) Electric dipole moments of the top quark

A term $\sim F_2\sigma_{\mu\nu}q_\nu\gamma_5$ can only be generated in a $\mathcal{CP}$ non-invariant electromagnetic or Z interaction. The static limit d of F_2 is the electric dipole moment of the top quark. Independently of the $\mathcal{CP}$ properties of the $t \to bW$ decay amplitude, such a contribution would be signalled by a non-zero expectation value of the $\mathcal{CP}$-odd momentum tensor [15] $T_{ij} = (q_+ - q_-)_i(q_+ \times q_-)_j/|q_+ \times q_-|$. The greatest sensitivity is achieved by choosing the unit momentum vectors of the charged W-decay leptons for $q_\pm$

$$\langle T_{ij}\rangle = \frac{\sqrt{s}}{e}\left[c_\gamma d^\gamma + c_Z d^Z\right] \cdot \mathrm{diag}\left[-\frac{1}{6}, -\frac{1}{6}, +\frac{1}{3}\right] \tag{2}$$

where the coefficient c_γ, for instance, falls rapidly from zero at threshold to ~ -0.4 at $\sqrt{s} = 500$ GeV for $m_t = 150$ GeV. Correlations between $q_+ \times q_-$ and the initial e^+e^- beam direction can be exploited to disentangle d^γ from d^Z. For a top mass $m_t = 150$ GeV, the sensitivity limits to the electric dipole moments are $d^{\gamma,Z} < 2.8 \times 10^{-18}$ e cm at $\sqrt{s} = 500$ GeV. Other correlations, like $q_{e^+}[q_{e^+} \times q_b - q_{e^-} \times q_{\bar{b}}]$, and energy asymmetries can be defined that are sensitive to $\mathcal{CP}$ violation in the decay current [15].

(c) Chirality of the (t, b) decay current

The precise determination of the weak isospin quantum numbers of the b quark [16] does not allow for large deviations of the (t, b) decay current from the left-handed $\mathcal{SM}$ prescription. Nevertheless, since $V + A$ admixtures may grow with the masses of the quarks involved, it is necessary to check the chirality of the decay current directly. The l^+ energy distribution in the semileptonic decay $t \to bW^+ \to l^+\nu_l$ depends sensitively on the chirality of the current:

$$\frac{\mathrm{d}\Gamma}{\mathrm{d}x_l} \sim \begin{cases} x_l(1 - x_l) & \text{for } V - A \\ (x_l - \mu^2)(1 - x_l + \mu^2) & \text{for } V + A \end{cases} \tag{3}$$

where $\mu^2 = m_W^2/m_t^2$ and $\mu^2 < x_l = 2E_l/m_t < 1$ denotes the scaled l^+ energy. Since the b-quark mass has been neglected, the two distributions add up incoherently, weighted with the probabilities for the $V \mp A$ mixture. Any deviation from the standard $V - A$ current would lead to a stiffening of the l^+ energy spectrum and, in particular, to a non-zero distribution at the upper end-point. $V + A$ admixtures of about 10% can be probed experimentally.

2.1.2 Non-Standard Top Decays

The theoretical analysis of non-standard top decays is motivated by the large top quark mass which could allow for exciting novel decay modes. A few illustrative yet characteristic examples will be discussed below. They demonstrate the great potential of top production in e^+e^- collisions, even if the novel decay processes are fairly rare.

(a) Charged Higgs decay

Charged Higgs states $H^{\pm}$ appear in 2–doublet Higgs models in which out of the eight degrees of freedom three Goldstone bosons build up the longitudinal states of the vector bosons and three neutral and two charged states correspond to real physical particles. A strong motivation for such an extended Higgs sector [9] is provided by supersymmetry which requires the $\mathcal{SM}$ Higgs sector to be doubled in order to generate masses for the up and down–type fermions. In the minimal version of that model the masses of the charged Higgs particles are predicted to be larger than the W mass, mod. radiative corrections, $m(H^{\pm}) > m(W^{+})$.

If the charged Higgs mass is lighter than the top mass, the top quark may decay into H^{+} plus a b quark [9, 17],

$$t \to b + H^{+} \tag{4}$$

The coupling of the charged Higgs to the scalar (t, b) current is defined by the quark masses and the parameter $\mathrm{tg}\beta$, $J(b,t) \sim m_b \mathrm{tg}\beta \pm m_t \mathrm{ctg}\beta$. Motivated by grand unification, the parameter $\mathrm{tg}\beta$, ratio of the vacuum expectation values of the Higgs fields giving masses to up and down–type fermions, will be assumed to be bounded by $1 < \mathrm{tg}\beta < m_t/m_b \sim 30$.

The branching ratio of this novel Higgs decay mode is compared with the standard W decay mode in Fig. 3a. In the GUT motivated parameter range, the W decay mode is dominant; the Higgs decay branching ratio is in general small, yet large enough to be clearly observable [8]. The detection of this scalar decay channel is facilitated by the characteristic decay pattern of the charged Higgs bosons $H^{+} \to \tau^{+}\nu_{\tau}$ and $c\bar{s}$. Since $H^{\pm}$ bosons couple preferentially to down–type fermions for $\mathrm{tg}\beta > 1$, the τ decay mode wins over the quark decay mode thus providing a clear experimental signature. A first signal of top decays into charged Higgs particles would therefore be the breakdown of μ, e *vs.* τ universality in semileptonic top decays, Fig. 3b.

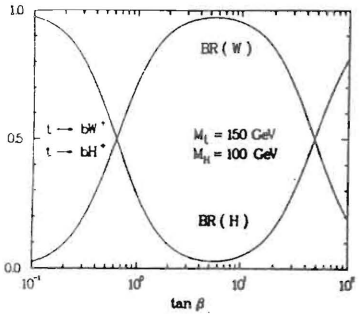

Fig. 3a Branching ratios for the decays $t \to bW^{+}$ and $t \to bH^{+}$ in two–doublet Higgs models [12].

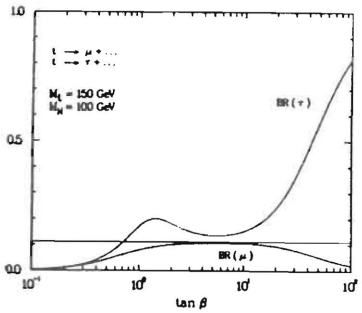

Fig. 3b Inclusive branching ratios for $t \to l + X$ and breaking of lepton universality. The value $\mathrm{BR}_l(t) = 1/9$ in the $\mathcal{SM}$ is indicated by the broken line [12].

(b) Top decay to stop

Another exciting decay mode in supersymmetry models is the decay of the top to the $\mathcal{SUSY}$ scalar partner stop plus neutralinos, mixtures of neutral gauginos and higgsinos [10]. This possibility is intimately related to the large top mass which leads to novel phenomena induced by the strong Yukawa interactions. These effects do not occur in light–quark systems but are special to the top system.

The mass matrix of the scalar $\mathcal{SUSY}$ partners $(\tilde{t}_L, \tilde{t}_R)$ to the left– and right–handed top–quark components (t_L, t_R) is built–up by the elements

$$\mathcal{M}^2 = \begin{Vmatrix} m^2_{\tilde{t}_L} + m_t^2 & \delta\tilde{m}^2_{LR} \\ \delta\tilde{m}^2_{LR} & m^2_{\tilde{t}_R} + m_t^2 \end{Vmatrix}$$

Large Yukawa interactions lower the diagonal matrix elements $\sim -m_t^2$ with respect to the common squark mass value in supergravity models, and they mix the $\tilde{t}_L$ and $\tilde{t}_R$ states with the strength $\sim m_t$ to form the mass eigenstates $\tilde{t}_1, \tilde{t}_2$. Unlike the five light quark species, these Yukawa interactions of $\mathcal{O}(m_t)$ can be so large in the top sector that after diagonalizing the mass matrix, the smaller eigenvalue may fall below the top quark mass, $m_{\tilde{t}_1} < m_t$. The decay modes, $t \to \tilde{t}+$ neutralinos then compete with the ordinary W decay mode. The ratio of the partial widths, $\Gamma(t \to \tilde{t}\tilde{\chi}^0_i)/\Gamma(t \to bW^{+})$ are in general less than 10% [10]. The subsequent t decays

$$\tilde{t} \to b\tilde{\chi}^{+}_i \ , \ \tilde{\chi}^{+}_i \to W\tilde{\chi}^0_1 \text{ or } l\tilde{\nu} \quad \text{or} \quad \tilde{t} \to c\tilde{\chi}^0_1 \ \ etc. \tag{5}$$

lead to an overall softer l spectrum and, as a result of the escaping photinos, to an increase of the missing energy, characteristic signature for $\mathcal{SUSY}$ induced phenomena [8].

(c) FCNC Decays

Within the $\mathcal{SM}$, FCNC decays like $t \to cZ$ are forbidden at the tree level by the GIM mechanism. However, they do occur in principle at the one–loop level, though strongly suppressed. The suppression is particularly severe for top decays since the quarks building up the loops, must be down–type quarks with m_b^2 setting the scale of the decay amplitude, $\Gamma_{FCNC} \sim \alpha G_F^2 m_b^4 m_t$, leading to branching ratios below 10^{-7}. At this level, no $\mathcal{SM}$ generated t decays can be observed. On the other hand, if these decay modes were detected, they would be an undisputed signal of new physics. From such options we select one illustrative example for direct GIM breaking [11].

The GIM mechanism requires all L and R quark components of the same electric charge in different families to carry identical isospin quantum numbers, respectively. This rule is broken by adding quarks in LR symmetric vector representations to the "light" chiral representations or mirror quarks. Depending on the specific form of the mass matrix, mixing between the normal chiral states and the new states may occur at the level $\sim (m/M)^{1/2}$, so that FCNC (t, c) couplings of the order $\sim (m_t m_c/M^2)^{1/2}$ can be induced. FCNC decays of top quarks, for example, with $\mathrm{BR}(t \to cZ) \sim$ fraction of % are therefore not excluded. Such branching ratios would be at the lower edge of the range accessible at $e^{+}e^{-}$ colliders.

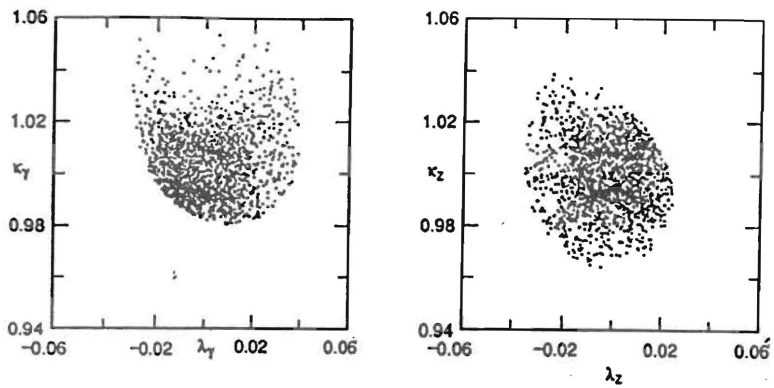

Fig. 4a Projections onto the $(\kappa_\gamma, \lambda_\gamma)$ and (κ_Z, λ_Z) planes of the 95% CL joint probability ellipsoid for a four parameter fit. $\sqrt{s} = 500$ GeV and $\mathcal{L} = 10$ fb^{-1} are assumed; from Ref. [18].

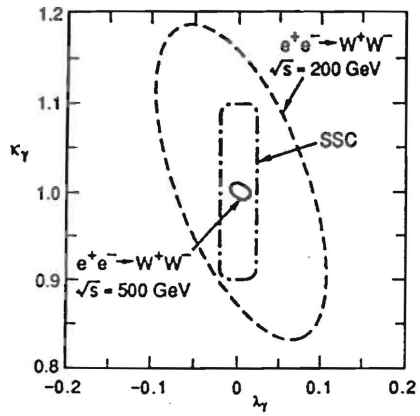

Fig. 4b Projections onto the $(\kappa_\gamma, \lambda_\gamma)$ plane of the 95% CL joint probability ellipsoid. $\mathcal{SM}$ values are assumed for (κ_Z, λ_Z) in the e^+e^- analysis; this assumption can be avoided at the expense of slightly larger integrated luminosities. Luminosities of $\int \mathcal{L} = 10$ fb^{-1} at $\sqrt{s} = 500$ GeV, $\int \mathcal{L} = 1.3$ fb^{-1} at $\sqrt{s} = 200$ GeV and $\int \mathcal{L} = 10$ fb^{-1} at the SSC are assumed; from Ref. [18].

These bounds, Fig. 4a, follow from the combined analysis of the W pair production cross section and the angular distributions of the W decay products which allow to separate the various W helicity components. To disentangle γ from Z couplings in this reaction, longitudinal beam polarization is essential. With beamstrahlung included properly, the bounds are based on an integrated luminosity of 10 fb^{-1}.

The bounds on $|\kappa_\gamma - 1|$ and $|\lambda_\gamma|$ that can be reached at e^+e^- linear colliders are compared with the values expected at the SSC from the measurement of the $W\gamma$ cross section in Fig. 4b. The e^+e^- linear colliders, even at $\sqrt{s} = 500$ GeV, are apparently more powerful by not only probing κ_γ and λ_γ to a higher accuracy, but by providing also stringent bounds on the Z coulings κ_Z and λ_Z.

2.2.2 Quartic Couplings

While the measurements of the triple couplings probe possible deviations from the non-abelian gauge symmetries due to novel interactions, the quartic couplings can provide a window to mechanisms of the electroweak symmetry breaking other than the light Higgs scenario of the $\mathcal{SM}$. New $WWWW$ couplings, for instance, can be induced by the exchange of heavy scalar particles.

The analysis of quartic couplings is still in the first phase of theoretical-phenomenological estimates [29]. Possible deviations from the quartic couplings prescribed by the gauge symmetries, are in general restricted to globally SU(2)$_W$ invariant interactions. For example,

$$(A) \ \dim = 4 \ : \ \mathcal{L}_4^0 = \frac{1}{4} g_0 g_W^2 (\vec{W}_\mu \vec{W}_\mu)^2 \ , \ \mathcal{L}_4^c = \frac{1}{4} g_c g_W^2 (\vec{W}_\mu \vec{W}_\nu)^2$$

These interactions give rise to $WWWW, WWZZ$ and $ZZZZ$ couplings which can be probed in the reactions

$$e^+e^- \longrightarrow W^+W^-Z \ \text{ and } \ ZZZ \tag{12}$$

Since these 3-particle cross sections are much smaller than those for W pair production, the bounds on quartic anomalies are correspondingly weaker, $|g_0| \leq 0.2$ and $|g_c| \leq 0.3$.

$$(B) \ \dim = 6 \ : \ \mathcal{L}_6^0 = -\frac{\pi\alpha}{4\Lambda^2} a_0 \vec{W}_\mu^2 F_{\nu\rho}^2 \ , \ \mathcal{L}_6^c = -\frac{\pi\alpha}{4\Lambda^2} a_c (\vec{W}_\mu F_{\mu\rho})^2$$

[F is the electromagnetic field]. These anomalous couplings can be measured in reactions such as

$$e^+e^- \to W^+W^-\gamma \ \text{ and } \ ZZ\gamma \tag{13}$$

The highest sensitivity however, can be achieved in the colliding $\gamma\gamma$ process

$$\gamma\gamma \to ZZ \tag{14}$$

[which is forbidden in the $\mathcal{SM}$ at tree level]: $|a_0| < 3 \times 10^{-3}$ and $|a_c| < 6 \times 10^{-3}$ for $\Lambda = M_W$. The energy scale which can effectively be probed, $M_W/\sqrt{a}$, is of the order of a TeV.

2.2 W, Z Interactions

The gauge symmetries of the Standard Model determine the form and the strength of the self-interactions of the electroweak bosons, triple couplings $WW\gamma, WWZ$ and quartic couplings $WWWW, WWZZ$ and $WW\gamma\gamma$. Deviations from the gauge symmetry values of these vertices, as well as novel couplings like ZZZ or $ZZ\gamma\gamma$ in addition to the canonical $\mathcal{SM}$ couplings could be expected in more general scenarios. In models with composite W, Z bosons for instance, corrections could alter the vertices to order $M_W/\Lambda_{\rm comp}$ and induce new types of couplings. Other examples are provided by models in which the W, Z bosons are generated dynamically or interact strongly with each other. While the experimental analysis of the self-couplings of the electroweak bosons can be carried out at collider energies of 500 GeV with high accuracy [18, 19, 20], WW scattering can only be studied at $\mathcal{O}$(TeV) energies [6, 18, 21]. This is a very important process to be investigated when light Higgs particles do not exist and W bosons become strongly interacting particles at high energies. We shall not discuss this alternative to the canonical $\mathcal{SM}$ in the present context but refer the reader to recent reviews on the subject.

2.2.1 Triple Couplings

The couplings $W^+W^-\gamma$ and W^+W^-Z are, in general, described by seven parameters each. Assuming $\mathcal{C}, \mathcal{P}$ and $\mathcal{T}$ invariance in the pure boson sector, the number of parameters can be reduced to three, which may be defined as

$$\begin{aligned}
\mathcal{L}_\gamma/g_\gamma &= ig_\gamma^1 W^+_{\mu\nu}W^\mu A^\nu + \text{h.c.} + i\kappa_\gamma W^+_\mu W^-_\nu F_{\mu\nu} + i\frac{\lambda_\gamma}{M_W^2}W^+_{\rho\mu}W_{\mu\nu}F_{\nu\rho} \\
\mathcal{L}_Z/g_Z &= ig_Z^1 W^+_{\mu\nu}W^\mu Z^\nu + \text{h.c.} + i\kappa_Z W^+_\mu W^-_\nu Z_{\mu\nu} + i\frac{\lambda_Z}{M_W^2}W^+_{\rho\mu}W_{\mu\nu}Z_{\nu\rho} \qquad (6)
\end{aligned}$$

While g_γ^1 and g_Z^1 are the electric and Z charges of the W bosons, the coefficients $\kappa_{\gamma,Z}$ and $\lambda_{\gamma,Z}$ are related to the corresponding magnetic dipole moments and electric quadrupole moments of the W bosons,

$$\begin{aligned}
\mu_\gamma &= \frac{e}{2M_W}(1+\kappa_\gamma+\lambda_\gamma) \quad \text{and} \quad [\gamma \to Z] \\
Q_\gamma &= -\frac{e}{M_W}(\kappa_\gamma-\lambda_\gamma) \quad \text{and} \quad [\gamma \to Z] \qquad (7)
\end{aligned}$$

The gauge symmetries of the $\mathcal{SM}$ demand $g_{\gamma,Z}=1$, and $\kappa_{\gamma,Z}=1$ and $\lambda_{\gamma,Z}=0$ for the anomalous moments at tree level.

Symmetries of the underlying dynamical interactions may constrain the generalized couplings. For example [22]

- (A) local $SU(2)_I$ symmetry : $\lambda_\gamma=\lambda_Z=\lambda$ and $\kappa_\gamma=\kappa_Z=1$
- (B) no intrinsic $SU(2)_I$ violation and no quadratic energy terms : $\kappa_\gamma \neq 1$ and $g_\gamma^1=1, \lambda_\gamma=\lambda_Z=0, \kappa_Z=1-(\kappa_\gamma-1)\text{tg}\theta_W, g_Z^1=-\text{tg}^2\theta_W+\kappa_\gamma/\cos^2\theta_W$

Bounds on the anomalous moments can be derived from high-precision measurements of electroweak observables which are affected by W-loop corrections. These effects have

been discussed for the Z boson parameters [23] and for atomic parity violation [24]. While some combinations of the couplings can be studied very well, blind directions prevent a general and comprehensive analysis.

The magnetic dipole and the electric quadrupole moments can be measured *directly* through the production of electroweak bosons at $p\bar{p}/pp$ and e^+e^- colliders. Modifications of the self-coupling vertices destroy the unitarity cancellations in the $\mathcal{SM}$ between interfering boson and fermion exchange amplitudes for longitudinal gauge boson production. As a result, small deviations of the moments from their $\mathcal{SM}$ values are magnified by a coefficient $\beta_W^2 s/M_W^2$, so that a 500 GeV e^+e^- collider will have a sensitivity which is more than one order of magnitude greater than LEP200. The clean experimental environment of e^+e^- colliders allows for a very high reconstruction efficiency of W bosons, so that e^+e^- linear colliders are competitive even with multi-TeV hadron colliders.

The analysis of $W\gamma$ final states at $p\bar{p}$ colliders led to bounds of $\mathcal{O}(1)$ for the anomalous photonic couplings. From the $W\gamma$ production cross sections at the future proton colliders LHC/SSC, bounds of order $|\lambda_\gamma| \leq 0.02$ and $|\kappa_\gamma - 1| \leq 0.1$ are expected [25], while information on λ_Z and κ_Z from WZ final states is more difficult to extract.

High energy e^+e^- colliders are ideal machines for probing the self-interactions of the electroweak gauge bosons. The main reaction to be exploited is W pair production [18, 22, 26]

$$e^+e^- \longrightarrow W^+W^- \qquad (8)$$

A large number $\mathcal{O}(10^6)$ of W pairs will be produced in a clean environment for the machine parameters specified above, so that high W reconstruction efficiencies can be achieved. Additional and complementary information can be obtained from the WW fusion to Z bosons [27]

$$e^+e^- \to \bar{\nu}\nu\,(WW) \to \bar{\nu}\nu Z \qquad (9)$$

and, in particular if laser induced γ beams are available, from [28]

$$\begin{aligned}
e^-\gamma &\to \nu W^- \\
\gamma\gamma &\to W^+W^- \qquad (10)
\end{aligned}$$

These processes are sensitive separately to γ and Z couplings so that they can help disentangle $\kappa_\gamma, \lambda_\gamma$ from κ_Z, λ_Z. Outstandingly tight bounds on the anomalous moments can be obtained [22, 26] if deviations from the $\mathcal{SM}$ values are constrained by the symmetry requirements (A) and (B) introduced above

$$\begin{aligned}
(A) \quad \lambda_\gamma=\lambda_Z &= -0.010 \;\to\; +0.002 \\
(B) \quad \kappa_\gamma - 1 &= -0.014 \;\to\; +0.000
\end{aligned}$$

If all κ_i and λ_i are allowed to vary freely, the anomalous moments can be probed [18] to an accuracy of

$$|\kappa_\gamma - 1|\,,\ |\kappa_Z - 1|\,,\ |\lambda_\gamma|\,,\ |\lambda_Z| \ \leq 0.02 \qquad (11)$$

3 Extensions of the Standard Model

3.1 Extended Gauge Theories

Despite of its tremendous success in describing the experimental data within the range of energies available today, the Standard Model based on the gauge symmetry SU(3) × SU(2) × U(1) is widely believed not to be the *ultima ratio*. Besides the fact that it has too many parameters which are merely incorporated by hand, the $\mathcal{SM}$ does not unify the electroweak and strong forces in a satisfactory way since the coupling constants of these interactions are different and appear to be independent. Therefore one would expect that a more fundamental theory exists which describes the three forces within the context of a single gauge group and hence, with only one coupling constant [30]. This grand unified theory will be based on a gauge group containing $SU(3)_C \times SU(2)_L \times U(1)_Y$ as a subgroup and will reduce to this symmetry at low energies.

Two predictions of grand unified theories can have dramatic phenomenological consequences in the energy range of a few hundred GeV:

i) The unifying group must be spontaneously broken at the unification scale, $\Lambda_{GUT} > 10^{15}$ GeV in order to be compatible with the experimental bounds on the proton lifetime. However, it is possible that the breaking to the $\mathcal{SM}$ group occurs in several steps and that some subgroups remain unbroken down to a scale of order 1 TeV. In this case the surviving group factors allow for new gauge bosons with masses not far from the scale of electroweak symmetry breaking.

ii) The grand unified groups incorporate fermion representations in which a complete generation of $\mathcal{SM}$ quarks and leptons can be naturally embedded. In most of the cases these representations are large enough to accomodate additional new fermions which are needed to have anomaly-free theories. It is conceivable that these new fermions [for instance, if they are protected by symmetries] acquire masses not much larger than the Fermi scale. This is very likely, and even necessary if the predicted new gauge bosons are relatively light.

The direct search for these new fermions and gauge bosons and tests of indirect effects [31] will be a major goal of the next generation of accelerators.

Besides the SU(5) group which has no room for "light" new gauge bosons or new fermions [the simplest Lie group containing SU(3)×SU(2)×U(1) as a subgroup and two representations to accomodate the 15 $\mathcal{SM}$ fermions], two other unifying groups have received much attention in recent years, SO(10) [32] and the exceptional group E_6 [33].

SO(10) is the simplest group in which the 15 Weyl spinors of each $\mathcal{SM}$ generation of fermions can be embedded into a single multiplet. This representation has dimension **16** and, in order to be anomaly-free, contains a right-handed neutrino

$$\begin{bmatrix} \nu_e \\ e \end{bmatrix}_L \quad e_R \quad \begin{bmatrix} u \\ d \end{bmatrix}_L \quad \begin{matrix} u_R \\ d_R \end{matrix} \quad ; \quad \nu_{eR} \tag{15}$$

The gauge group can be spontaneously broken to the $\mathcal{SM}$ group at an intermediate scale, two interesting chains of breaking patterns being via SU(5)×U(1) or SU(4)× SU(2)×SU(2),

leading to the intermediate symmetries [32]

$$\begin{aligned} SO(10) \rightarrow \quad & SU(3)_C \times SU(2)_L \times U(1)_Y \times U(1)_\chi \quad \rightarrow SU(3)_C \times SU(2)_L \times U(1)_Y \\ \rightarrow \quad & SU(3)_C \times SU(2)_L \times SU(2)_R \times U(1)_{B-L} \quad \rightarrow SU(3)_C \times SU(2)_L \times U(1)_Y \end{aligned} \tag{16}$$

These chains would induce new right-handed charged currents and/or neutral currents which could eventually be studied at TeV energies.

Another popular unifying group is E_6. It contains SU(5) and SO(10) as subgroups and is the next anomaly-free choice after SO(10). The interest in this group is mainly due the fact that superstring theories, which attempt to unify all fundamental forces including gravity, suggest this theory as a possible four dimensional field theoretic limit [34]. In E_6, each quark-lepton generation lies in a representation of dimension **27**. To complete this representation, twelve new fields are needed in addition the $\mathcal{SM}$ fermion fields. For each family one has two additional isodoublets of leptons, two isosinglet neutrinos and an isosinglet quark with charge −1/3,

$$\begin{bmatrix} \nu_E \\ E \end{bmatrix}_L \quad \begin{bmatrix} \nu_E \\ E \end{bmatrix}_R \quad n \quad n' \quad D_L \quad D_R \tag{17}$$

In the breaking of E_6 down to the $\mathcal{SM}$ gauge group, two additional U(1) symmetry factors may survive at low energies [33]

$$\begin{aligned} E_6 \rightarrow SO(10) \times U(1)_\psi \quad & \rightarrow \quad SU(5) \times U(1)_\chi \times U(1)_\psi \\ & \rightarrow \quad SU(3)_C \times SU(2)_L \times U(1)_Y \times U(1)_\chi \times U(1)_\psi \end{aligned} \tag{18}$$

leading to two new neutral gauge bosons. Assuming that only one of them is light, the relevant neutral gauge boson would be $Z' = Z_\chi \cos\beta + Z_\psi \sin\beta$, where β=0 and $\pi/2$ correspond to pure Z_χ and Z_ψ while $\beta = \mathrm{arctg}(-\sqrt{5/3})$ corresponds to the model η in which E_6 is directly broken to a rank-5 group at the unification scale in superstings models [34].

Several other gauge groups have been considered, based on various theoretical motivations. For instance, schemes of grand unification built-up on large orthogonal groups have been proposed to explain the origin of parity violation in weak interactions [35]. In these models, weak interactions are $\mathcal{P}$ invariant but fermions with left-handed and right-handed couplings aquire different masses. They predict a new spectrum of fermions, mirror fermions [36], which have chiral properties opposite to the ordinary particles. In the simplest version of these models, the gauge symmetry and the symmetry breaking pattern are the same as in the Standard Model; three families of heavy fermions with opposite chiralities are simply added to the $\mathcal{SM}$ spectrum

$$\begin{bmatrix} N_R \\ E_R \end{bmatrix} \quad \begin{matrix} N_L \\ E_L \end{matrix} \quad \begin{bmatrix} U_R \\ D_R \end{bmatrix} \quad \begin{matrix} U_L \\ D_L \end{matrix} \tag{19}$$

Theoretical arguments based on [weak coupling] unitarity [37] suggest that the masses of these mirror fermions should not exceed a few hundred GeV.

3.1.1 New Gauge Bosons

The existence of an extra neutral gauge boson with a mass below the maximal energy of the e^+e^- collider will provide a new resonance which will increase the e^+e^- annihilation cross section by several orders of magnitude. In this case, an e^+e^- collider operating at the resonance peak would be a "Z' factory" allowing to measure the couplings of the Z' to other conventional and new particles with very high precision, a situation comparable to the LEP experiments exploring the Z peak. High-energy e^+e^- colliders would then be ideal instruments to study the properties of the new gauge bosons and to constrain the theories predicting their origin.

Even if a new vector boson is too heavy to be produced as a resonance, it could give rise to virtual effects which are measurable. Indeed, besides mixing with the Z, a new heavy Z' will participate in the production process of ordinary fermions [38, 39]

$$e^+e^- \longrightarrow \gamma, Z, Z' \longrightarrow f\bar{f} \tag{20}$$

and it will affect the cross sections and the various asymmetries through its propagator effects. The clean environment of e^+e^- colliders allows to probe these virtual effects with high precision and therefore provides a sensitivity to Z' masses considerably higher than the available center of mass energy. In addition, because of the number of observables which can be measured precisely, a detailed investigation of the properties of the new Z' boson can be performed and its origin can be identified.

The virtual effects of a new Z' associated with the most general effective theories which arise from the breaking of E_6, $SU(3)_C \times SU(2)_L \times U(1)_Y \times U(1)_{Y'}$ and $SU(2)_L \times SU(2)_R \times U(1)$, have been investigated in Ref. [39]. Assuming that the Z' is heavier than the c.m. energy, its propagator effects on various observables of the process $e^+e^- \to f\bar{f}$ have been studied. Since the effects of the new Z' are expected to be rather small, one has to include radiative corrections which can mimic the signal. Taking into account the backgrounds [e.g. from W pair production $e^+e^- \to W^+W^-$ and two photon-events $e^+e^- \to e^+e^-f\bar{f}$], a number of observables which are most sensitive to the new Z' effects were selected. The leptonic cross section and the forward-backward asymmetry $\sigma^{\rm lep}$ and $A_{FB}^{\rm lep}$, the ratio of the hadronic and leptonic cross section $R = \sigma^{\rm lep}/\sigma^{\rm had}$ as well as the polarization asymmetries $A_{LR}^{\rm had}$ and $A_{LR}^{\rm lep}$ were shown to be best suited to probe high Z' masses and to discriminate between various models.

Assuming an integrated luminosity of 20 fb^{-1} and a cut on the final state fermion energy $\Delta = 0.7$, Fig. 5a demonstrates that when combining the measurements of $\sigma^{\rm lep}$, $A_{FB}^{\rm lep}$ and $R = \sigma^{\rm lep}/\sigma^{\rm had}$, the effects of the new Z' can be probed for masses up to 3 TeV at the 95% confidence level without polarization [thick solid curve]. Assuming that longitudinal polarization is available, this value can be extended up to 3.5 TeV for certain values of the model parameters [thick dotted curve]. In the ideal case of vanishing systematic errors [thin curves], Z' masses up to 4 TeV can be probed for certain parameter values. An excellent distinction between extra U(1) and left-right models can be obtained for Z' masses below 1.5 TeV. Fig. 5b shows that only a small confusion region [the hatched area] remains in this case. The increase of the sensitivy if polarization is available, is very important since in this case the confusion region [cross hatched area] becomes much

smaller. Finally, the determination of the model parameters themselves is also possible up to masses of similar size.

At pp colliders, Z' discovery limits range up to 3–5 TeV at the LHC and up to 5–6 TeV at the SSC [40]. However, due to the difficult environment, the identification of the origin of the Z' will probably be limited to masses below 1 to 2 TeV. If a new Z' with such a mass is found at LHC/SSC, a 500 GeV e^+e^- collider would give valuable complementary information on its detailed properties.

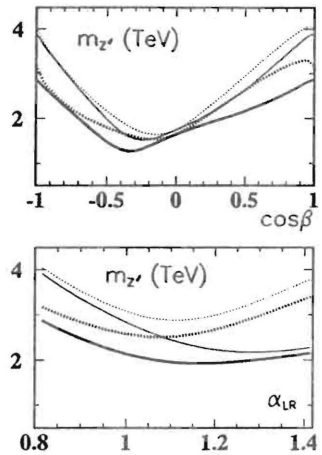

Fig. 5a Z' mass limits in models with an extra U(1) and left-right models. Solid (dotted) lines: without (with) polarization.

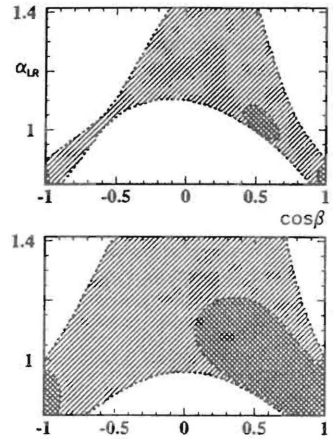

Fig. 5b Distinction between models with an extra U(1) and left-right models. Top (bottom): $M_{Z'}$ =1.5 (2) TeV.

3.1.2 New Fermions

The new leptons and quarks will mix with the ordinary fermions of the Standard Model. The mixing will give rise to new currents which determine to a large extent their decay properties, and allow for new production mechanisms [41]. LEP data restrict the mixing angles to values smaller than $\mathcal{O}(10^{-1})$ [42] and the masses of new states [except for the singlet neutrinos] to values larger $M_Z/2$ [43]. For mixing angles close to the upper limit, the mass range between $M_Z/2$ and M_Z is also excluded. [This range will also be probed through pair production at LEP200.]

If the new particles have non-zero electromagnetic and weak charges, they can be pair produced if their masses are smaller than the beam energy of the e^+e^- collider [41, 44, 45]. In general, the reactions are built-up by a superposition of γ and Z exchange, but additional contributions could come from the extra neutral bosons if their masses are not much larger than the c.m. energy. At a 500 GeV collider, the cross sections are fairly

large [44, 45], up to phase space suppression factors, of the order of the point-like QED cross section $\sigma(e^+e^- \to F\overline{F}) \sim \sigma_0 \simeq 400$ fb. This leads to samples of several thousands events for a luminosity $\mathcal{L} = 10^{33}$ cm^{-2}s^{-1}. The large number of events allows to probe masses up to the kinematical limit of 250 GeV. In some cases, the singlet neutrinos can be produced with sufficient rates if a Z' boson with a mass below 1 TeV exists. The cross sections for E_6 lepton pair production at $\sqrt{s} = 500$ GeV are shown in Fig. 6a in units of σ_0, $R_L = \sigma(e^+e^- \to L\overline{L})/\sigma_0$; the solid lines are the predictions in the limit of a very heavy Z' [the cross sections for mirror leptons are of similar size] while the dashed lines include the contribution of the extra SO(10) Z' with a mass of 700 GeV. For a heavy Z', the zero-values of the forward-backward asymmetries of E_6 leptons clearly indicate the vectorial nature of their couplings; the forward-backward asymmetries of mirror leptons are of opposite sign to those of fourth generation leptons.

Fermion mixing allows an additional production mechanism for the new fermions: single production in association with their light partners. In this case, masses very close to the total energy of the e^+e^- collider can be reached. For the second and third generation of leptons [if inter-generational mixing is neglected] and for quarks, the process proceeds only through s-channel Z exchange and leads to relatively small cross sections. But in the case of the first generation leptons, additional t-channel exchanges [W exchange for neutral leptons and Z exchange for charged leptons] are present, increasing the cross sections by several orders of magnitude. The cross sections [44] are shown in Fig. 6b for E_6 leptons at $\sqrt{s} = 500$ GeV, with the left and right-handed mixing angles set to $\zeta_L, \zeta_R = 0.1$ i.e. close to the upper limit. In the case of the first generation neutral and charged leptons, the important contributions of the t-channel Z or W exchanges result in large production cross sections, allowing the discovery of these particles up to masses close to 500 GeV. The production cross sections for the leptons of the second and third generations $L^{2,3}$ [and for quarks] are much smaller; they will nevertheless provide direct information, for the first time, on the mixing angles in these families.

For masses larger than M_Z, the new fermions will decay into ordinary fermions and on-shell weak bosons. At e^+e^- colliders, the signals are clear and rather easy to separate from backgrounds due to conventional processes. Once these particles have been found, the clean environment allows the detailed investigation of their properties: measurement of their masses, determination of their couplings and quantum numbers. Angular distributions and the polarization of the heavy final states can be exploited to discriminate between particles of different nature [e.g. Majorana or Dirac neutrinos] or with different couplings [e.g. vector or standard chiral couplings in pair production, or with left or right-handed mixing in single production].

At hadron colliders, strongly interacting new particles can be produced with very large cross sections. However, because of large backgrounds, the detailed investigation of the basic properties of these particles is difficult, contrary to e^+e^- colliders which are well suited for such high-precision analyses. Because of the backgrounds, the search for new leptons with masses larger than $\mathcal{O}(M_Z)$ is also difficult at pp colliders [46]. On the other hand, at e^+e^- colliders new leptons can be discovered easily up to masses close to the beam energy, and even to the total energy if their mixing is large enough. In this respect, e^+e^- colliders are complementary to the pp colliders.

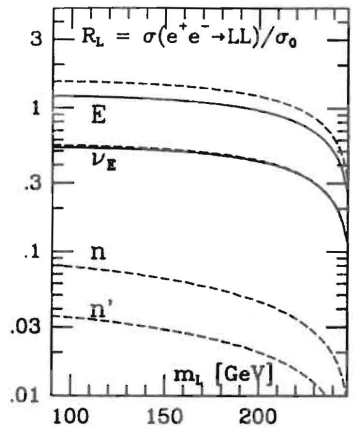

Fig. 6a Cross sections for the pair production of E_6 leptons in units of σ_0. The solid (dashed) lines correspond to $M_{Z'} = \infty$ ($M_{Z'} = 700$ GeV).

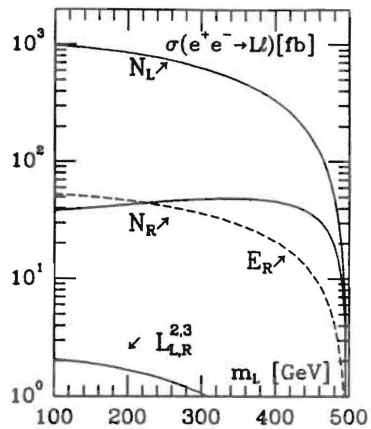

Fig. 6b Cross sections for the single production of E_6 leptons. N standards generically for ν_E, n and n'.

3.2 Supersymmetry

Supersymmetric theories are very attractive extensions of the Standard Model. They provide a theoretical framework in which the problems of naturalness and hierarchy in the Higgs sector are solved, while retaining the Higgs bosons as elementary particles with moderate masses in the context of high energy scales demanded by unification. The Minimal Supersymmetric extension of the Standard Model ($\mathcal{MSSM}$) [47, 9] may serve as a useful guideline into this area. The model is characterized by the gauge group SU(3)×SU(2)×U(1) and the requirement of minimal particle content. This minimal theory led to a prediction for $\sin^2\theta_W$ that is in very nice agreement with present high-precision measurements of the electroweak mixing angle [48].

The particle content of the model consists of the $\mathcal{SM}$ particles, gauge bosons, quarks and leptons, yet with an extended two-doublet Higgs sector, plus their supersymmetric partners, gauginos and Higgsinos [partly mixing to form charginos and neutralinos] and the scalar squarks and sleptons. The low energy energy $\mathcal{SUSY}$ sector is described by five basic parameters if the theory is embbeded into a grand unified theory: the universal scalar mass m_0, the SU(2) gaugino mass M, the mass parameter μ in the Higgs sector, the mass of the lightest Higgs boson M_h and tgβ, the ratio of the vacuum expectation values of the two Higgs fields.

3.2.1 The Higgs Sector

Supersymmetry requires the existence of at least two iso-doublet scalar fields Φ_1 and Φ_2. The $\mathcal{MSSM}$ is restricted to this minimal extension. The field Φ_2 (with vacuum expectation value v_2) couples only to up-type quarks while Φ_1 (with vacuum expectation value v_1) couples to down-type quarks and charged leptons. Five physical Higgs bosons are introduced in this theory: two $\mathcal{CP}$-even neutral bosons h and H (where h will be considered to be the lightest particle), a $\mathcal{CP}$-odd neutral boson A (usually called pseudoscalar) and two charged Higgs bosons $H^{\pm}$. Besides the four masses M_h, M_H, M_A and $M_{H^{\pm}}$, two additional parameters define the properties of the scalar particles and their interactions with gauge bosons and fermions: the ratio of the two vacuum expectation values $\mathrm{tg}\beta = v_2/v_1$ and a mixing angle α in the neutral $\mathcal{CP}$-even sector. Supersymmetry leads to several relations among these parameters and, in fact, only two of them are independent. These relations impose a strong hierarchical structure on the mass spectrum $[M_h < M_Z, M_A < M_H$ and $M_W < M_{H^{\pm}}]$ which however is broken by radiative corrections if the top quark mass is large [49]. The parameter $\mathrm{tg}\beta$ will in general be assumed in the range $1 < \mathrm{tg}\beta < \mathrm{m_t}/\mathrm{m_b}$ $[\pi/4 < \beta < \pi/2]$, consistent with the GUT constraints on the model.

(a) Parameters and Decay Modes

Since the lightest $\mathcal{CP}$-even Higgs boson h is likely to be the particle which will be discovered first, an attractive choice of the two input parameters is the set $[M_h, \mathrm{tg}\beta]$, with $\mathrm{tg}\beta$ parametrizing the production cross sections. Once these two parameters [as well as the top quark mass and the associated squark masses which enter through radiative corrections] are specified, all other masses $M_H, M_A, M_{H^{\pm}}$ and the angle α can be derived.

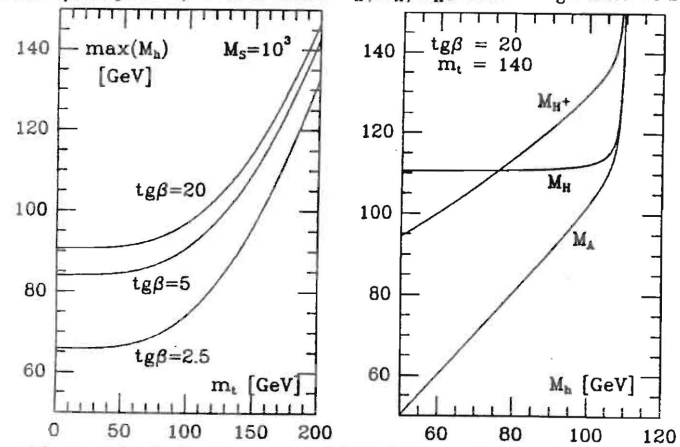

Fig. 7 Masses of the $\mathcal{SUSY}$ Higgs bosons. (a) Max(M_h) as a function of m_t and (b) M_H, M_A and $M_{H^{\pm}}$ as functions of M_h for $m_t = 140$ GeV. The squark masses M_S are fixed to 1 TeV.

The radiative corrections grow as the fourth power of the top quark mass m_t and logarithmically with the squark mass M_S. They are positive and they shift the mass of the light neutral Higgs boson h upward with increasing top mass. The variation of the upper limit of M_h with the top quark mass is shown in Fig. 7a for $M_S = 1$ TeV and three representative values of $\mathrm{tg}\beta = 2.5, 5$ and 20. The upper bound on M_h is shifted from the tree level value M_Z up to ~ 130 GeV for $m_t = 180$ GeV. Assuming [from now on] that $m_t = 140$ GeV and $M_S = 1$ TeV, the masses M_A, M_H and $M_{H^{\pm}}$ are depicted in Fig. 7b, as a function of the light neutral Higgs mass for $\mathrm{tg}\beta = 20$. Apart from the range near the upper limit of M_h for fixed $\mathrm{tg}\beta$, the mass values cluster in characteristic bands of 100 to 150 GeV for M_H and $M_{H^{\pm}}$, and up to ~ 100 GeV for M_A. On general grounds, the masses of the heavy neutral and charged Higgs bosons are expected to be of the order of the electroweak symmetry breaking scale so that a large part of the Higgs mass spectrum can be explored in e^+e^- colliders with a total energy of 300 to 500 GeV [50, 51].

The couplings of the various neutral Higgs bosons to fermions and gauge bosons will in general depend on the angles α and β. Normalized to the $\mathcal{SM}$ Higgs couplings, they are summarized in Tab. 1 and Fig. 8. The pseudoscalar A does not have tree-level couplings to gauge bosons, and its couplings to down (up) type fermions are (inversely) proportional to $\mathrm{tg}\beta$. The couplings depend in general strongly on the input parameters $\mathrm{tg}\beta$ and M_h. The couplings to down (up) type fermions are enhanced (suppressed) compared to the $\mathcal{SM}$ Higgs couplings. If M_h is very close to its upper limit for a given value of $\mathrm{tg}\beta$, the couplings to fermions and gauge bosons are $\mathcal{SM}$ like. If all other Higgs bosons are very heavy, it is very difficult to distinguish the Higgs sector of the $\mathcal{MSSM}$ from the $\mathcal{SM}$.

Φ	$g_{\Phi\bar{u}u}$	$g_{\Phi\bar{d}d}$	$g_{\Phi VV}$
h	$\cos\alpha/\sin\beta$	$-\sin\alpha/\cos\beta$	$\sin(\beta-\alpha)$
H	$\sin\alpha/\sin\beta$	$\cos\alpha/\cos\beta$	$\cos(\beta-\alpha)$
A	$1/\mathrm{tg}\beta$	$\mathrm{tg}\beta$	0

Tab.1 Higgs couplings in the $\mathcal{MSSM}$ to fermions and gauge bosons relative to $\mathcal{SM}$ couplings.

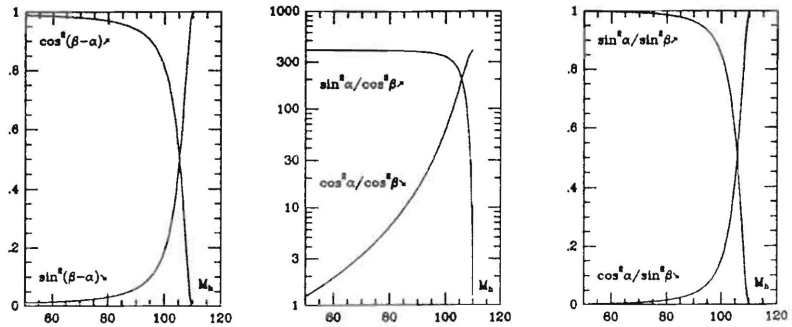

Fig. 8 H and h couplings to fermions and gauge bosons as a function of M_h for $\mathrm{tg}\beta = 20$.

The lightest neutral Higgs boson will decay mainly into fermion pairs since its mass is smaller than $\sim$ 130 GeV. This is also the dominant decay mode of the pseudoscalar boson A which has no tree-level couplings to gauge bosons. For values of tgβ larger than unity and for masses less than $\sim$ 140 GeV, the main decay modes of the neutral Higgs bosons are decays into $b\bar{b}$ and $\tau^+\tau^-$ pairs; the branching ratios being always larger than $\sim$ 90% and 5%, respectively. The decays into $c\bar{c}$ pairs and gluons [which proceeds through t and b quark loops] are strongly suppressed especially for large tgβ. For large masses, the top decay channels $H, A \to t\bar{t}$ open up; yet this mode remains suppressed for large tgβ.

If the mass is high enough, the heavy $\mathcal{CP}$-even Higgs boson can in principle decay into weak gauge bosons $H \to VV$, $V = W$ or Z. Since the partial widths are proportional to $\cos^2(\beta - \alpha)$, they are strongly suppressed and the gold-plated ZZ signal of the heavy $\mathcal{SM}$ Higgs boson is lost in the supersymmetric extension. [If M_H is large enough for these decay modes to be kinematically allowed, M_h is very close to its maximum value so that $\cos^2(\beta - \alpha) \to 0$.] For the same reason, the cascade decay of the $\mathcal{CP}$-odd Higgs boson, $A \to Zh$, is suppressed in general. The heavy neutral Higgs boson H can also decay into two lighter Higgs bosons. These modes, however, are restricted to very small domains in the parameter space. Decays into $\gamma\gamma$ and $Z\gamma$ final states are very rare and do not play a significant role at e^+e^- colliders.

Other possible channels are decays into supersymmetric particles [52]. While sfermions are likely too heavy to affect Higgs decays in the mass range considered here, Higgs boson decays into charginos and neutralinos could eventually be important since some of these particles are expected to be of the order of M_Z. These new channels are kinematically accessible at least for the heavy Higgs bosons H, A and $H^\pm$; in fact, the branching fractions can be very large and they can even be dominant in some regions of the $\mathcal{MSSM}$ parameter space. Decays of h into the lightest neutralinos and charginos are also important, exceeding 50% in some corners of the $\mathcal{SUSY}$ parameter space. These decays will affect experimental searches. In particular, neutral Higgs decays into the lightest neutralinos which would be invisible, are important and they could jeopardize the search for the Higgs particles at hadron colliders where these decays are very difficult to find. At e^+e^- colliders however, missing mass techniques allow to isolate these events easily, at least for the $\mathcal{CP}$-even Higgs bosons which can be produced in association with the Z boson.

The coupling of the charged Higgs particles to fermions is a $\mathcal{P}$ violating mixture of scalar and pseudoscalar currents. The charged Higgs particles decay into fermions but also, if allowed kinematically, into the lightest neutral Higgs and a W boson. Below the tb and Wh thresholds, the charged Higgs particles will decay mostly into $\tau\nu_\tau$ and $c\bar{s}$ pairs, the former being dominant for tg$\beta > 1$. For large $M_{H^\pm}$ and tgβ values, the top-bottom decay mode $H^+ \to t\bar{b}$ becomes dominant.

Adding up the various decay modes, the width of all five Higgs bosons remains very narrow, being of the order of 1 GeV even for large masses. Apart from the $\mathcal{CP}$-even heavy neutral Higgs boson H and small values of tgβ, the pattern of branching ratios is in general quite simple if supersymmetric decays are ignored. The neutral Higgs bosons decay preferentially to $b\bar{b}$, and to a lesser extent to $\tau^+\tau^-$ pairs; the charged Higgs bosons to $\tau\nu_\tau$ and, preferentially, to $t\bar{b}$ pairs above the threshold. These decay patterns lead to clear signatures for the detection of these particles in e^+e^- colliders.

(b) Production

The search for the neutral $\mathcal{SUSY}$ Higgs bosons at 500 GeV e^+e^- colliders will be a direct continuation of the search to be performed at LEP200. This collider is expected to cover the mass range up to $\sim$ 85 GeV for neutral Higgs bosons. Higher energies, $\sqrt{s} > 240$ GeV, are required to sweep the entire parameter space of the $\mathcal{MSSM}$. The main production mechanisms of neutral Higgs bosons at e^+e^- colliders [53] are the bremsstrahl process and pair production,

$$
\begin{array}{lll}
(a) \text{ bremsstrahlung} & e^+e^- \to (Z) \to Z + h/H \\
(b) \text{ pair production} & e^+e^- \to (Z) \to A + h/H
\end{array}
$$

as well as the fusion processes,

$$
\begin{array}{lll}
(c) \text{ fusion processes} & e^+e^- \to \nu\,\bar{\nu}\,(WW) \to \nu\,\bar{\nu} + h/H \\
 & e^+e^- \to e^+e^-(ZZ) \to e^+e^- + h/H
\end{array}
$$

The $\mathcal{CP}$-odd Higgs boson A cannot be produced in fusion processes to leading order.

The cross sections for the four bremsstrahl and pair production processes can be expressed as [53]

$$
\begin{aligned}
\sigma(e^+e^- \to Zh) &= \sin^2(\beta - \alpha)\,\sigma_{SM} \\
\sigma(e^+e^- \to ZH) &= \cos^2(\beta - \alpha)\,\sigma_{SM} \\
\sigma(e^+e^- \to Ah) &= \cos^2(\beta - \alpha)\,\sigma_{SM}\,\bar{\lambda} \\
\sigma(e^+e^- \to AH) &= \sin^2(\beta - \alpha)\,\sigma_{SM}\,\bar{\lambda}
\end{aligned}
\tag{21}
$$

where σ_{SM} is the $\mathcal{SM}$ cross section for Higgs bremsstrahlung and the factor $\bar{\lambda}$ accounts for the correct suppression of the P-wave cross sections near the threshold. The cross sections for the bremsstrahlung and for the pair production as well as the cross sections for the production of the light and the heavy neutral Higgs bosons h and H are mutually complementary to each other, coming either with a coefficient $\sin^2(\beta - \alpha)$ or $\cos^2(\beta - \alpha)$. Since σ_{SM} is large [54], at least the lightest $\mathcal{CP}$-even Higgs boson can be detected [50, 51]. Depending on the values of M_h and tgβ, the following final states will be observed [Fig. 9]:

$$
\begin{array}{llllll}
M_h \text{ "small"}, & \text{tg}\beta \text{ small}: & hZ, & HZ, & hA, & HA \\
 & \text{tg}\beta \text{ large}: & & HZ, & hA, & \\
M_h \text{ "large"}, & \text{tg}\beta \text{ small}: & hZ, & & & [HA] \\
 & \text{tg}\beta \text{ large}: & hZ, & & & [HA]
\end{array}
$$

where "M_h small" and "large" are synonymous for "considerably below" and "close to the upper limit of the light $\mathcal{CP}$-even Higgs boson" for a given value of tgβ. If M_h is "large" the H, A masses can exceed the kinematical limit for HA pair production. In the part of the $\mathcal{MSSM}$ parameter space in which invisible h decays into neutralinos are important, the bremstrahl cross section is large so that missing mass techniques can be applied.

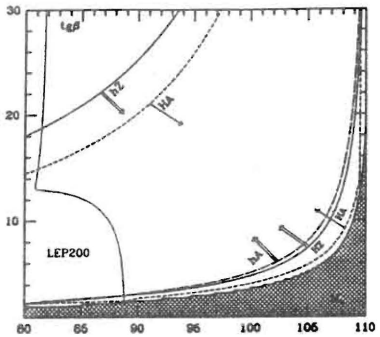

Fig. 9 Regions of the $(M_h, \mathrm{tg}\beta)$ plane where the four cross sections (21) are larger than 2.5 fb [25 events for $\int \mathcal{L} = 10$ fb^{-1}]. The dashed area is the theoretically forbidden region. The thin lines are the regions which can be probed at LEP200 [25 events at $\sqrt{s}$ = 180 GeV and $\int \mathcal{L} = 500$ pb^{-1}.]

The cross sections for the various production mechanisms of the neutral Higgs bosons are shown as functions of the Higgs mass in Fig. 10, for $\mathrm{tg}\beta = 20$; Ref. [50, 52] . The cross section for hZ is large for large values of M_h where it is of the order of $\sim$ 50 fb, corresponding to $\sim$ 500 events for an integrated luminosity of 10 fb^{-1}. By contrast, the cross section for HZ is large for light h [implying small M_H]. In the case of h [and also for H in most of the parameter space] the signal consists of a Z boson accompanied by a $b\bar{b}$ or a $\tau^+\tau^-$ pair. The signal is easy to separate from the background which comes mainly from ZZ production if the Higgs mass is close to M_Z. For the associated channels $e^+e^- \to Ah$ and AH, the situation is opposite to the previous case: the cross section for Ah is large for light h whereas AH production is preferred in the complementary region. The sum of the two cross sections decreases from $\sim$ 50 to 10 fb if M_A increases from $\sim$ 50 to 200 GeV. In major parts of the parameter space, the signals consist of four b quarks in the final state, requiring facilities for efficient b quark tagging. Mass constraints will help to eliminate the backgrounds from QCD jets as well as ZZ final states. For the WW fusion mechanism, the cross sections are larger than for the bremsstrahl process if the Higgs mass is moderately small – less than 160 GeV at $\sqrt{s}$ = 500 GeV. However, since the final state cannot be fully reconstructed, the signal is more difficult to extract. As in the case of the bremsstrahl process, the production of light h and heavy H Higgs bosons are complementary. The cross sections for the ZZ fusion mechanism are about an order of magnitude smaller than for the WW fusion process. ZZ fusion will nevertheless be useful since the final state can be fully reconstructed.

The preceding discussion of the neutral $\mathcal{MSSM}$ Higgs sector at e^+e^- linear colliders can be summarized in the following points:

(i) The lightest $\mathcal{CP}$–even Higgs particle h can be detected in the entire range of the $\mathcal{MSSM}$ parameter space, either through the bremsstrahl process $e^+e^- \to hZ$ or through pair production $e^+e^- \to hA$. In fact, this conclusion holds true even at a c.m. energy of 300 GeV, independently of the top and squark mass values, and also if invisible neutralino decays are allowed for.

(ii) There is a substantial area of the $[M_h, \mathrm{tg}\beta]$ parameter space where *all* neutral $\mathcal{SUSY}$ Higgs bosons can be discovered at a 500 GeV collider. This is possible if the masses of the heavy scalar H and the pseudoscalar A boson are less than $\sim$ 230 GeV.

(iii) In some part of the $\mathcal{MSSM}$ parameter space, the lightest Higgs particle h can be detected, but it cannot be distinguished from the $\mathcal{SM}$ Higgs boson. This happens if, for a given value of $\mathrm{tg}\beta$, M_h is very close to its maximum and H and A are too heavy to be produced in association. In this case, the couplings of h to gauge bosons and fermions are $\mathcal{SM}$ like. As long as this ambiguity cannot be resolved by proceeding to higher collider energies, the only way to distinguish h from the $\mathcal{SM}$ Higgs particle is provided by Higgs production in $\gamma\gamma$ fusion. While this process is built–up by W and top quark loops in the $\mathcal{SM}$, additional contributions in $\mathcal{SUSY}$ models are provided by supersymmetric particle loops, such as charginos, which alter the $\mathcal{SM}$ production rates.

Some of these features are not specific to the minimal extension but they are expected to be realized also in more general $\mathcal{SUSY}$ models. For example, a light Higgs boson with a mass in the intermediate range is predicted in supersymmetric theories quite generally.

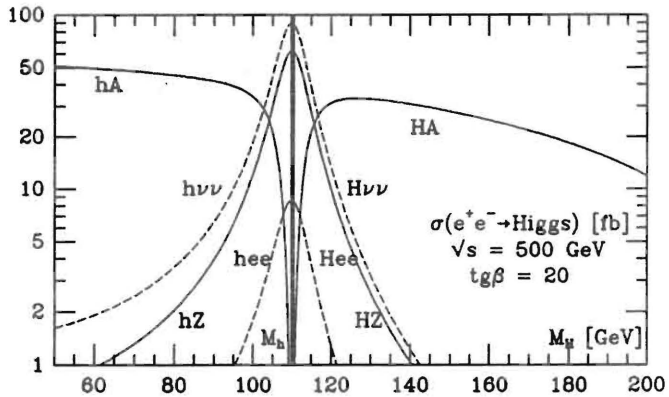

Fig. 10 Production cross sections of the $\mathcal{SUSY}$ neutral Higgs bosons in e^+e^- collisions as function of the masses [in GeV] for $\mathrm{tg}\beta = 20$.

In the $\mathcal{MSSM}$, the mass of the charged Higgs bosons $H^\pm$ is constrained to be larger than that of the W boson. More precisely, the lower limit $M_h > 60$ GeV obtained at LEP100 [43] implies $M_{H^\pm} > 100$ GeV. In e^+e^- collisions, the production of a pair of charged Higgs bosons proceeds through virtual photon and Z boson exchange. The cross section depends only on the charged Higgs mass [and does not depend on any extra parameter]. For small Higgs masses the cross section is of order 100 fb, but it drops very quickly due to the P–wave suppression factor β^3 near the threshold; Fig. 11. For $M_{H^\pm} = 220$ GeV,

the cross section has fallen to a level of $\simeq 5$ fb, which for an integrated luminosity of 10 fb^{-1} corresponds to 50 events. The angular distribution of the charged Higgs bosons follows the $\sin^2\theta$ law typical for spin-zero particle production. Charged Higgs particles can also be created in $\gamma\gamma$ collisions. Generating the γ beams through back-scattering of laser light, the total energy of the $\gamma\gamma$ collider can go up to $\sim 80\%$ of the original e^+e^- energy, which corresponds to $\sqrt{s_{\gamma\gamma}} \simeq 400$ GeV for a 500 GeV e^+e^- collider. Due to the reduced energy, the maximum Higgs mass which can be probed in $\gamma\gamma$ collisions, is smaller than the limit at the original e^+e^- collider; the cross section however is enhanced by a factor ~ 3 in the low mass range [Fig. 11].

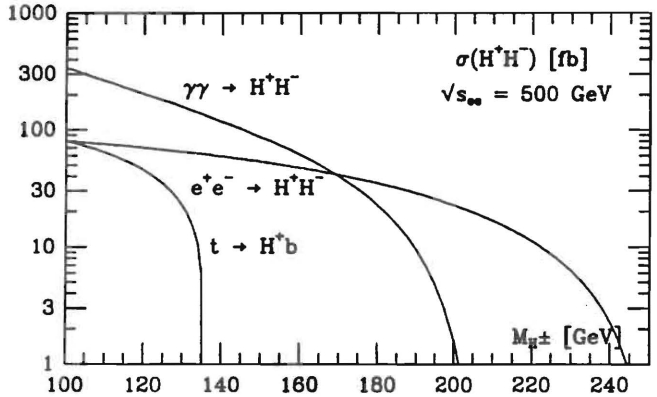

Fig. 11 Production cross sections of the charged Higgs bosons in e^+e^- and $\gamma\gamma$ collisions as well as from top decays [for $m_t = 140$ GeV and tg$\beta = 20$].

The charged Higgs boson, if lighter than the top quark, can also be produced in top decays as discussed above. In the range $1 < \text{tg}\beta < m_t/m_b$ favored by $\mathcal{SUSY}$ models, the branching ratio varies between $\sim 2\%$ and 20%. Since the cross section for top pair production is of order 0.5 pb at $\sqrt{s} = 500$ GeV, this corresponds to 200 and 2000 charged Higgs bosons at a luminosity $\int \mathcal{L} = 10$ fb^{-1}. If $M_{H^\pm} < m_t + m_b$, the charged Higgs boson will decay mainly into $\tau\nu_\tau$ and $c\bar{s}$ pairs, the $\tau\nu_\tau$ mode dominating for tgβ larger than unity. This results in a surplus of τ final states over e, μ final states in t decays, an apparent breaking of τ *vs.* e, μ universality. For large Higgs masses the dominant decay mode is the top decay $H^+ \to t\bar{b}$. In some part of the parameter space also the decay $H^+ \to W^+h$ is allowed, leading to cascades with heavy τ and b particles in the final state.

3.2.2 Supersymmetric Particles

a) Charginos and Neutralinos

The two charginos $\tilde{\chi}_i^+$ and the four neutralinos $\tilde{\chi}_i^0$, mixtures of the [non-colored] gauginos and Higgsinos, are expected to be the lighthest supersymmetric particles [55]. To avoid unnatural fine-tuning in radiative corrections, the masses of the particles are expected in the range below the Fermi scale [55]. In the $\mathcal{MSSM}$ with conserved R-parity, the neutralino $\tilde{\chi}_1^0$ with the smallest mass, assumed to be the lightest supersymmetric particle altogether, is stable. The heavier neutralinos and the charginos decay into (possibly virtual) gauge and Higgs bosons plus $\tilde{\chi}_1^0$,

$$\begin{aligned} \tilde{\chi}_i^0 &\longrightarrow \tilde{\chi}_1^0 + Z \;;\; \tilde{\chi}_1^0 + h, H \text{ or } A \\ \tilde{\chi}_i^+ &\longrightarrow \tilde{\chi}_1^0 + W \;;\; \tilde{\chi}_1^0 + H^+ \end{aligned} \tag{22}$$

or, if they are heavy enough, into cascades of neutralinos/charginos plus gauge and Higgs bosons. In the same way the heavy charginos decay into $\tilde{\chi}_1^+$ and W or $H^\pm$ bosons, *etc.*

Neutralinos and charginos are difficult to find at hadron colliders, but they are easy to detect at e^+e^- colliders [56, 57]. They are produced in pairs

$$\begin{aligned} e^+e^- &\longrightarrow \tilde{\chi}_i^+ + \tilde{\chi}_j^+ \qquad [i,j = 1,2] \\ e^+e^- &\longrightarrow \tilde{\chi}_i^0 + \tilde{\chi}_j^0 \qquad [i,j = 1,..,4] \end{aligned} \tag{23}$$

through s-channel γ, Z exchange and t-channel selectrons or sneutrinos exchange. The kinematically accessible $\mathcal{SUSY}$ parameter range in the $[M, \mu]$ plane is shown in Fig. 12, for the different chargino and neutralino production processes at a 500 GeV e^+e^- collider [58]. Compared to the region which can be explored by LEP200, a substantial extension can be expected. Since the cross sections are as large as $\mathcal{O}(100$ fb), enough events will be produced to discover these particles and to study their properties. It has been demonstrated, in fact, by detailed experimental simulations that these particles can be found with masses up to the beam energy of e^+e^- colliders, if the mass difference $m(\tilde{\chi}) - m(\tilde{\chi}_1^0)$ is not less than about 20 GeV.

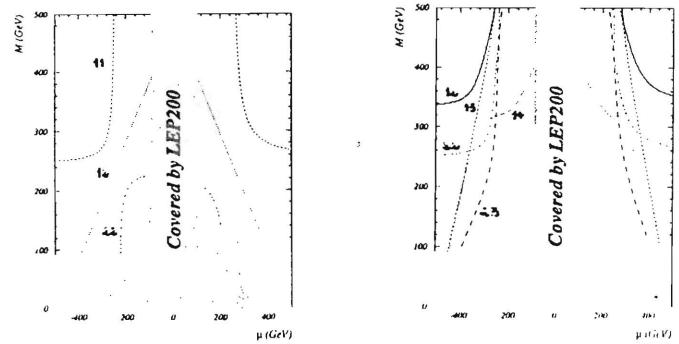

Fig. 12 Regions of the $[\mu, M]$ plane for tg$\beta = 4$ where the processes $e^+e^- \to \tilde{\chi}_i^+\tilde{\chi}_j^-$ and $e^+e^- \to \tilde{\chi}_i^0\tilde{\chi}_i^0$ are kinematically accessible at $\sqrt{s} = 500$ GeV. The numbers ij correspond to $\tilde{\chi}_i\tilde{\chi}_j$ combinations; from Ref. [58].

b) Sleptons

Left or right-handed scalar particles $\tilde{f}_L$ or $\tilde{f}_R$ correspond to each chiral $\mathcal{SM}$ fermion. Starting with a universal scalar mass m_0^2 at the GUT scale, squark and slepton masses evolve differently down to low energies. Slepton masses are expected to be significantly smaller than squark masses, and they may have values near the scale of electroweak symmetry breaking.

The superpartners of the right-handed leptons decay into the associated partner and neutralinos. In major parts of the $\mathcal{SUSY}$ parameter space the dominant decay mode is $\tilde{e}_R \to e\tilde{\chi}_1^0$. For the superpartners of the left-handed sleptons, the decay pattern is slightly more complicated since besides the $\tilde{\chi}_1^0$ channels, decays into leptons and charginos are also possible [58]. In e^+e^- collisions, sleptons are produced pairwise [58]

$$\begin{aligned} e^+e^- &\longrightarrow \tilde{e}_L^+\tilde{e}_L^- \,,\ \tilde{e}_R^+\tilde{e}_R^- \,,\ \tilde{e}_L^+\tilde{e}_R^- \,,\ \tilde{e}_R^+\tilde{e}_L^- \\ e^+e^- &\longrightarrow \tilde{\nu}_L\bar{\tilde{\nu}}_L \\ e^+e^- &\longrightarrow \tilde{\mu}_L^+\tilde{\mu}_L^- \,,\ \tilde{\mu}_R^+\tilde{\mu}_R^- \,,\ \tilde{\tau}_L^+\tilde{\tau}_L^- \,,\ \tilde{\tau}_R^+\tilde{\tau}_R^- \end{aligned} \tag{24}$$

For charged sleptons, the production proceeds via γ, Z exchange in the s-channel. In the case of selectrons, an additional t-channel neutralino exchange, which is also responsible for the creation of the mixed left and right-handed selectron states, is present. For sneutrinos, the process is mediated by s-channel Z-exchange and in the case of electron-sneutrinos also by t-channel exchange of charginos.

The cross sections for the pair production of smuons (stau's) and their neutral partners are shown in Fig. 13. Again, smuons can be discovered up to the kinematical limit if the mass difference $m(\tilde{\mu}) - m(\tilde{\chi}_1^0)$ is not smaller than a few tens of GeV [59]. Similar results have been obtained for selectrons for which the cross sections are larger because of additional contributions from t-channel neutralino exchange [60]. Though not investigated in detail yet, sneutrinos should also be found readily at e^+e^- colliders.

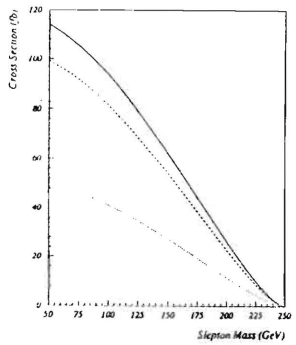

Fig. 13 The total cross sections [in fb] for slepton pair production at $\sqrt{s}$ = 500 GeV as a function of the mass; from [58].
$e^+e^- \to \tilde{\mu}_L^+\tilde{\mu}_L^-$ (solid)
$e^+e^- \to \tilde{\mu}_R^+\tilde{\mu}_R^-$ (dashed)
$e^+e^- \to \tilde{\nu}_\mu\bar{\tilde{\nu}}_\mu$ (dotted).

Selectrons can also be produced in association with photinos [$\sim \tilde{\chi}_1^0$] in $e\gamma$ collisions, $e\gamma \to \tilde{e}\tilde{\chi}_1^0$ [61]. For small photino masses, the kinematic range of the selectron mass extends beyond the $e^\pm$ beam energy. However, it seems difficult to exploit this window in practice, since for masses beyond the $e^\pm$ beam energies the rates are quite low.

While colored squarks [and gluinos] can be detected up to masses of $\mathcal{O}$(1 TeV), the slepton search at proton colliders, on the other hand, is very difficult due to the low production rates and the large backgrounds so that e^+e^- linear colliders are unique in this sector.

4 Conclusions

e^+e^- linear colliders operating in the energy range of 300 to 500 GeV [that can be expanded to 1 to 2 TeV] have a very high physics potential, complementary to that of proton colliders. High precision measurements in the top and the W, Z gauge boson sectors will not only lead to a deeper understanding of the Standard Model and its symmetry principles, but anomalous properties of these particles could hold important clues to the mechanism of the electroweak symmetry breaking and to elements of the physics beyond the Standard Model. Extended gauge symmetries suggest new vector bosons and novel exotic leptons which can be explored in e^+e^- colliders very well. Last but not least, these colliders provide unique facilities to explore central aspects of supersymmetric extensions of the Standard Model, the Higgs spectrum and its properties, the gaugino/Higgsino sector and the supersymmetric partners of the leptons.

The clarity of view given into the energy regime characterized by the scale of electroweak symmetry breaking, and the opportunities for exploring new physical phenomena beyond the Standard Model, make e^+e^- linear colliders unique facilities for addressing key issues at the frontier of fundamental physics.

References

[1] For recent reviews, see the reports by B. Richter, G. Voss and B. Wiik in Ref. [2].

[2] Proceedings of the "Workshop on Physics and Experiments with Linear e^+e^- Colliders", Saariselkä (Finland), World Scientific Publ. Comp., Singapore 1992.

[3] Proceedings of the Workshop "e^+e^- Collisions at 500 GeV: The Physics Potential", Munich-Annecy-Hamburg, DESY Report 92-123 A+B.

[4] W. Kozanecki [conv.] et al. in Ref. [3].

[5] V. Telnov in Ref. [2].

[6] M. E. Peskin in Ref. [2].

[7] G. Kane, G. A. Ladinsky and C. P. Yuan, Phys. Rev. D45 (1992) 124; C. P. Yuan Phys. Rev. D45 (1992) 782.

[8] P. Igo-Kemenes and J. H. Kühn [conv.] et al. in Ref. [3].

[9] For a review of the SUSY Higgs sector, see J. Gunion, H. Haber, G. Kane and S. Dawson, The Higgs Hunter's Guide, Addison-Wesley, Reading 1990.

[10] K. Hikasa and M. Kobayashi, Phys. Rev. D36 (1987) 724; H. Baer et al. Phys. Rev. D44 (1991) 725.

[11] W. Buchmüller and M. Gronau, Phys. Lett. B220 (1989) 641; H. Fritzsch, Phys. Lett. B224 (1989) 423.

[12] P. M. Zerwas in Ref. [2].

[13] E. Reya and P. M. Zerwas et al., Proceedings of the Large Hadron Collider Workshop, Aachen 1990, CERN 90-10.

[14] C. Schmidt and M. E. Peskin in Ref. [2].

[15] W. Bernreuther et al. in Ref. [3].

[16] D. Schaile and P. M. Zerwas, Phys. Rev. D45 (1992) 3262.

[17] G. L. Kane, Proceedings Madison Workshop 1979; I. Bigi, Y. Dokshitzer, V. Khoze, J. H. Kühn and P. M. Zerwas, Phys. Lett. B181 (1986) 157; C. S. Li and T. C. Yuan, Phys. Rev. D42 (1990) 3088.

[18] T. Barklow in Ref. [2].

[19] W. Beenakker, F. A. Behrends and A. Denner [conv.] et al. in Ref. [3].

[20] F. Boudjema and F. M. Renard [conv.] et al. in Ref. [3].

[21] K. Hikasa in Ref. [2].

[22] G. Gounaris, J. L. Kneur, J. Layssac, G. Moultaka, F. M. Renard and D. Schildknecht in Ref. [3].

[23] A. De Rujula et al., CERN-TH-6272-91; K. Hagiwara et al., Phys. Lett. B283 (1992) 353; C. Burgess and D. London, McGill 92-05 and 92-14.

[24] S. Godfrey, Phys. Rev. D45 (1992) 3196.

[25] G. Kane, J. Vidal and C. P. Yuan, Phys. Rev. D39 (1989) 2617.

[26] M. Frank, P. Mättig, R. Settles and W. Zeuner in Ref. [3].

[27] S. Ambrosanio and B. Mele in Ref. [3]; G. Couture, R. Lewis and S. Godfrey, Phys. Rev. D45 (1992) 777.

[28] E. Yehudai, Phys. Rev. D44 (1991); S. Choi and F. Schrempp in Ref. [3].

[29] G. Bélanger and F. Boudjema in Ref. [3]; J. Kalinowski in Ref. [3].

[30] H. Georgi and S. L. Glashow, Phys. Rev. Lett. 32 (1974) 438; J.C. Pati and A. Salam, Phys. Rev. D10 (1974) 275.

[31] A. Djouadi, D. Schaile and C. Verzegnassi [conv.] et al. in Ref. [3].

[32] R. Robinett and J. Rosner, Phys. Rev. D25 (1982) 3036; P. Langacker, R. Robinett and J. Rosner, Phys. Rev. D30 (1984) 1470; V. Barger et al., Phys. Lett. 118B (1982) 68.

[33] For a review of E_6, see J. L. Hewett and T. G. Rizzo, Phys. Rep. 183 (1989) 193.

[34] For a review, see J. Ellis, Proc. Workshop on Grand Unification, Icoban (Japan), 1986.

[35] J. C. Pati and A. Salam, Phys. Lett. 58B (1975) 333; G. Senjanovic, F. Wilczek and A. Zee, Phys. Lett. 141B (1984) 389.

[36] J. Maalampi and M. Roos, Phys. Rep. C186 (1990) 53; I. Montvay, Phys. Lett. 205B (1988) 315; F. Csikor and I. Montvay, Phys. Lett. 231B (1990) 503.

[37] M. Chanowitz, M. Furman and I. Hinchliffe, Phys. Lett. B78 (1978) 285; J. Bagger, S. Dimopoulos and E. Massó, Nucl. Phys. B253 (1985) 397.

[38] G. Bélanger and S. Godfrey, Phys. Rev. D34 (1986) 1309; U. Amaldi et al., Phys. Rev. D36 (1987) 1385; V. Barger et al., Phys. Rev. D37 (1987) 2893; J. L. Hewett and T. G. Rizzo, Z. Phys. C36 (1987) 209; G. Costa et al., Nucl. Phys. B297 (1988) 293; A. Blondel et al., Nucl. Phys. B331 (1990) 293.

[39] A. Djouadi, A. Leike, T. Riemann, D. Schaile and C. Verzegnassi in Ref. [3].

[40] P. Chiappetta, M. Greco et al., Proc. of the LHC Workshop, Aachen 1990, CERN 90-10; R. M. Barnett et al., Proceedings on the 1988 Snowmass Summer Study, 1988; J. Hewett and T. G. Rizzo, MAD/PH/645 (1991).

[41] W. Buchmüller in Ref. [2]; V. Barger et al., Phys. Rev. D33 (1986) 1912; T. G. Rizzo, Phys. Rev. D34 (1986) 1438; F. del Aguila, E. Laermann and P. M. Zerwas, Nucl. Phys. B297 (1988) 1; W. Buchmüller and C. Greub, Nucl. Phys. B363 (1991) 345.

[42] P. Langacker and D. London, Phys. Rev. D38 (1988) 244; W. Buchmüller, C. Greub and H. Kohrs, Nucl. Phys. B370 (1992) 3; E. Nardi, E. Roulet and D. Tommasini, FERMILAB PUB-91/207-A.

[43] M. Davier, Rapporteur Talk at the HEP Lepton–Photon Conference, Geneva 1991, Preprint LAL 91–48.

[44] A. Djouadi, M. Spira and P. M. Zerwas in Ref. [3].

[45] W. Buchmüller, C. Greub, P. Mikowski, M. Talbi and G. Tysarcszyk–Niemeyer in Ref. [3]; F. Csikor, A. Djouadi and I. Montvay in Ref. [3].

[46] V. Barger, T. Han and J. Ohnemus, Phys. Rev. D37 (1988) 1174; V. Barger and R. Phillips, Collider Physics, Addison Wesley, 1987.

[47] For reviews of supersymmetric theories, see P. Fayet and S. Ferarra, Phys. Rep. 32 (1977) 249; H. P. Nilles, Phys. Rep. 110 (1984) 1; H. Haber and G. Kane, Phys. Rep. 117 (1985) 75; R. Barbieri, Riv. Nuovo Cimento 11 (1988) 1.

[48] J. Ellis, S. Kelley and D. V. Nanopoulos, Phys. Lett. 260B (1991) 131; U. Amaldi, W. de Boer and H. Fürstenau, Phys. Lett. 260B (1991) 447; P. Langacker and M. Luo, Phys. Rev. D44 (1991) 817; G. G. Ross and R. G. Roberts, Preprint RAL–92–005.

[49] For a summary of radiative corrections, see F. Zwirner in Ref. [2].

[50] A. Djouadi, J. Kalinowski and P. M. Zerwas in Ref. [3].

[51] P. Janot in Ref. [3]; A. Brignole et al. in Ref. [3]; A. Yamada, UT–KOMABA–92–1 (1992); V. Barger, K. Cheung, R. Phillips and A. Stange, MAD–PH–696 (1992).

[52] J. Gunion and H. Haber, Nucl. Phys. B307 (1988) 445; A. Djouadi, J. Kalinowski and P. M. Zerwas, DESY 92–160; H. Baer et al., FSU–HEP–92–0724.

[53] J. F. Gunion et al., Phys. Rev. D38 (1988) 3444.

[54] A. Djouadi, D. Haidt, B. Kniehl, B. Mele and P. M. Zerwas in Ref. [3].

[55] R. Barbieri in Ref. [47]; G. G. Ross and R. G. Roberts in Ref. [48].

[56] A. Bartl and D. Treille [conv.] et al. in Ref. [3].

[57] J. F. Grivaz in Ref. [3].

[58] A. Bartl, W. Majerotto and B. Mösslacher in Ref. [3].

[59] R. Becker and R. Starosta in Ref. [3].

[60] C. Vander Velde in Ref. [3].

[61] D. Borden, D. Bauer and D. Caldwell, SLAC–PUB–5715 (1992); H. König and K. Petterson, OCIP–C–92–1; F. Cuypers, G. van Oldenborgh and R. Rückl, LMU–92–02.